ATLAS NOTE

20th March 2015

Statistical combination of all-hadronic and one-lepton analyses targeting scalar top pair production using proton-proton collisions at $\sqrt{s} = 8$ TeV with the ATLAS detector

The ATLAS Collaboration

ATLAS-CONF-2015-010
20 March 2015

Abstract

A statistical combination of two analyses targeting direct stop pair production and requiring respectively no leptons and one lepton in the final state is presented. The observed exclusion limit on the stop mass for a small neutralino mass in a scenario where the stop is assumed to decay only into $\tilde{t} \to t\tilde{\chi}_1^0$ is 700 GeV. This is an increase by about 50 GeV with respect to the limits obtained by the individual analyses. Limits are also presented when varying the branching fraction between the stop decaying by $\tilde{t}_1 \to t\tilde{\chi}_1^0$ and $\tilde{t}_1 \to b\tilde{\chi}_1^{\pm}$.

1 Introduction

In a theory with broken supersymmetry (SUSY) [1–9], the mass scale of the supersymmetric particles is undetermined. However, the additional assumption that SUSY provides a solution to the hierarchy problem [10–13] imposes constraints on the SUSY particle spectrum, suggesting that some of them have masses within the reach of the LHC [14, 15].

The scalar partner of the top quark (the stop) is among these particles. In a supersymmetric extension [16–20] of the Standard Model (SM), the large Yukawa coupling of the top quark to the Higgs sector makes the predictions at the electroweak scale sensitive to the masses of the stop states. The supersymmetric partners of the left-handed and right-handed top quark states ($\tilde{t}_L$ and $\tilde{t}_R$ respectively) mix to form the mass eigenstates $\tilde{t}_1$ and $\tilde{t}_2$ ($\tilde{t}_1$ being the lightest by definition).

The ATLAS [21] and CMS [22] collaborations have searched for the stop [23–38] using data from the proton-proton collisions produced by the LHC at $\sqrt{s} = 8$ TeV. These extensive searches have found no evidence for stop signals, leading to exclusion limits in many SUSY models.

The aim of this note is to provide a statistical combination of the analyses targeting stop pair production with final states containing either no leptons or one lepton[1] and described in Refs. [23] and [24] (referred to as t0L and t1L respectively in the following). The scenario considered assumes that the stop can decay into either $\tilde{t}_1 \to t\tilde{\chi}_1^0$, where $\tilde{\chi}_1^0$ is the lightest neutralino, or into $\tilde{t}_1 \to b\tilde{\chi}_1^\pm$, where $\tilde{\chi}_1^\pm$ is the lightest chargino (a mass of the lightest chargino of $m_{\tilde{\chi}_1^\pm} = 2m_{\tilde{\chi}_1^0}$, motivated by gauge universality considerations, is assumed here). Sketches of the relevant diagrams are shown in Figure 1. It is also assumed that the mass of the stop exceeds the sum of that of the top quark and the neutralino, such that the decay $\tilde{t}_1 \to t\tilde{\chi}_1^0$ is always kinematically allowed. The event selections of the t0L and t1L analyses are mutually exclusive and provide a comparable sensitivity to these scenarios, hence making a statistical combination meaningful.

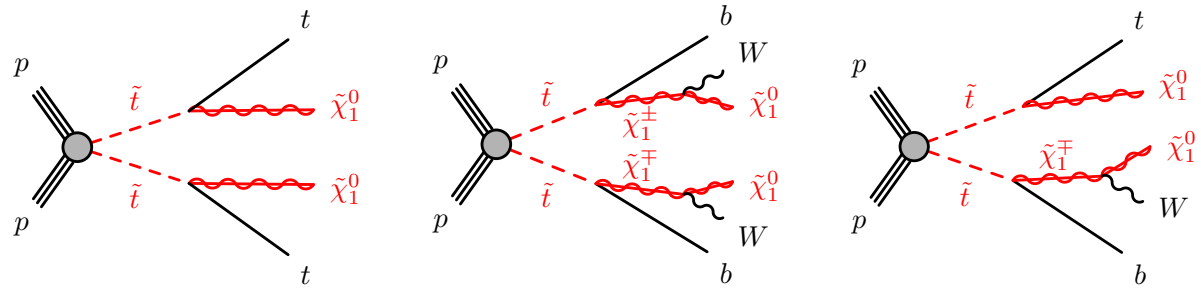

(a) $\tilde{t}_1\tilde{t}_1 \to t\tilde{\chi}_1^0 t\tilde{\chi}_1^0$ (b) $\tilde{t}_1\tilde{t}_1 \to b\tilde{\chi}_1^\pm b\tilde{\chi}_1^\pm$ (c) $\tilde{t}_1\tilde{t}_1 \to b\tilde{\chi}_1^\pm t\tilde{\chi}_1^0$

Figure 1: Diagrams for $\tilde{t}_1$ pair production followed by the decay of the stop into $\tilde{t}_1 \to t\tilde{\chi}_1^0$ or $\tilde{t}_1 \to b\tilde{\chi}_1^\pm$.

After a quick review of the general analysis strategy (in section 2) and a brief summary (in section 3) of the t0L and t1L event selections, the procedure adopted for the combination, and the results obtained are described in section 4.

[1] The analysis requiring two leptons in the final state of Ref. [25] is not included in the combination, given the lower sensitivity to the scenarios considered.

2 General analysis strategy

The two analyses used in the statistical combination presented in this note share a common analysis strategy and common statistical techniques, which are described in Ref. [39].

Signal regions (SRs) are defined, which target one specific model and SUSY mass parameter set. Their event selections are optimised by relying on the Monte Carlo simulation of both the SM background production processes and the signal. No use of the observed event yields is made during this step. The optimisation process aims to maximise the expected sensitivity to the models considered, and takes into account the possible interplay of different signal regions.

For each SR, multiple control regions (CR) are defined to constrain the normalisation of the most relevant SM production processes. The event selections of the CRs are mutually exclusive, and they are such that the event yield is dominated by one specific background process. The event yields in the CRs, together with the MC expectations both in the CRs and SRs, are used to estimate the SM background composition from the CRs into the SRs.

A likelihood function is built as the product of Poisson probability functions, describing the observed and expected numbers of events in the control and signal regions. The observed numbers of events in the various CRs are used to determine the normalisation parameters for the dominant background processes, thus generating internally consistent SM background estimates for each of the SRs via a profile likelihood fit. Systematic uncertainties are treated as nuisance parameters in the fit and are constrained with Gaussian functions. The fit procedure takes into account correlations in the yield predictions between different regions due to common background normalisation parameters and systematic uncertainties, as well as contamination from SUSY signal events in the CRs, when a particular model is considered for exclusion.

The full procedure is validated by comparing the background predictions from the fit results and the shapes of the distributions of the key analysis variables to the observed event yields and shapes in dedicated validation regions (VRs), which are defined to be kinematically similar to the signal regions while keeping the possible signal contamination under control.

After successful validation, the observed yields in the signal regions are compared to the predictions. The profile likelihood ratio test-statistic [40] is used first to compare the data to the SM background-only hypothesis, and then to exclude the signal plus background hypothesis in specific signal models. A signal model is said to be excluded at 95% confidence level (CL) if the CL_s [41, 42] of the test-statistic of the signal plus background hypotheses is below 0.05.

3 Experimental Signatures

The discussion of the t0L and t1L analyses is reduced to a reminder for sake of brevity. Table 1 summarises the full list of signal regions defined by the analyses, together with the model targeted and the references to the corresponding published papers.

Table 1: List of the signal regions defined by the t0L and t1L analyses, together with the SUSY model that they target.

Analysis name and corresponding reference	Original signal region name	Model targeted
All-hadronic states [23] - t0L	SRA1-SRA4, SRB SRC1-SRC3	$\tilde{t}_1 \to t\tilde{\chi}_1^0$ $\tilde{t}_1\tilde{t}_1 \to t\tilde{\chi}_1^0 b\tilde{\chi}_1^\pm$ with $m_{\tilde{\chi}_1^\pm} = 2m_{\tilde{\chi}_1^0}$
One lepton final states [24] - t1L	tN_diag tN_med, tN_high, tN_boost bCa_low, bCa_med, bCb_med1, bCb_high, bCb_med2, bCc_diag, bCd_bulk, bCd_high1, bCd_high2 3body tNbC_mix	$\tilde{t}_1 \to t\tilde{\chi}_1^0$ with $m_{\tilde{t}_1} \sim m_{\text{top}} + m_{\tilde{\chi}_1^0}$ $\tilde{t}_1 \to t\tilde{\chi}_1^0$ $\tilde{t}_1 \to b\tilde{\chi}_1^\pm$ $\tilde{t}_1 \to bW\tilde{\chi}_1^0$ (3-body decay) $\tilde{t}_1\tilde{t}_1 \to bt\tilde{\chi}_1^0\tilde{\chi}_1^\pm$ with $m_{\tilde{\chi}_1^\pm} = 2m_{\tilde{\chi}_1^0}$

All-hadronic final states The analysis has been designed to be sensitive to final states arising from all-hadronic decays of pair produced stops [23]. Two sets of signal regions have been optimised to maximise the sensitivity to topologies arising from $\tilde{t}_1 \to t\tilde{\chi}_1^0$ decays, assumed to occur with a branching ratio of one. The first set of signal regions, named t0L-SRA, assumes that both top quark hadronic decays can be fully resolved by making use of six anti-k_t jets with $R = 0.4$. The signal is extracted from the SM background (dominated by $t\bar{t}$ and Z+ heavy flavour jets production) based on the presence of two hadronic systems consistent with top quarks and large missing transverse momentum. The second signal region, named t0L-SRB, targets a similar scenario, but aims at signal topologies where the top quarks have a large boost. Designed to select final states with four of five $R = 0.4$ anti-k_t jets to be mutually exclusive with t0L-SRA, the event selection relies on the presence of $R = 0.8$ and $R = 1.2$ anti-k_t jets containing the hadronic decay products of the two top quarks: their masses, together with other variables including transverse mass variables computed with the missing transverse momentum and jets in the event are used as discriminant against the dominant SM $t\bar{t}$, Z + jets and W + jets production background processes.

Finally, a third set of signal regions, named t0L-SRC, has been designed to increase the analysis sensitivity to decays in which the stop decays into $\tilde{t}_1 \to b\tilde{\chi}_1^\pm$. These signal regions require five anti-k_t jets with $R = 0.4$, and they are based on a set of transverse mass variables aimed at rejecting the dominant SM $t\bar{t}$ production process.

One lepton final states The large number of signal regions defined by this analysis stems from the variety and complexity of the possible stop final states considered [24]. All signal regions are characterised by the presence of one lepton (electron or muon), a veto on other leptons, a minimum of two jets and a large amount of missing transverse momentum. A first set of signal regions have been optimised assuming a branching ratio of 100% for the decay $\tilde{t} \to t\tilde{\chi}_1^0$. The four signal regions aim at having sensitivity to different $\Delta m(\tilde{t}, \tilde{\chi}_1^0)$, with t1L-tN_diag targeting compressed scenarios and making full use of the shape

information of the $E_{\mathrm{T}}^{\mathrm{miss}}$ and m_{T} distributions[2] to maximise the sensitivity in this difficult region. The t1L-tN_boost SR targets regions with the largest $\Delta m(\tilde{t}, \tilde{\chi}_1^0)$, where the top quark produced by the stop decay has a large boost: the use of large radius jets is the key ingredient to maximise the sensitivity in this region.

The decay $\tilde{t} \to \tilde{\chi}_1^{\pm} b$ introduces additional degrees of freedom in the decay. The final state kinematics is largely driven by the mass separation between the stop and the chargino $\Delta m(\tilde{t}, \tilde{\chi}_1^{\pm})$, and by that between the chargino and the neutralino $\Delta m(\tilde{\chi}_1^{\pm}, \tilde{\chi}_1^0)$. Several signal regions, identified by the prefix t1L-bC have been designed and optimised depending on the mass hierarchy. Four possible categories of mass hierarchies are considered: the first mass hierarchy is characterised by small values of both $\Delta m(\tilde{\chi}_1^{\pm}, \tilde{\chi}_1^0)$ and $\Delta m(\tilde{t}, \tilde{\chi}_1^{\pm})$, with soft leptons emitted in the chargino decay and soft b-jets arising from the stop decay vertex. A second hierarchy still considers compressed chargino-neutralino scenarios, but targets larger values of $\Delta m(\tilde{\chi}_1^{\pm}, \tilde{\chi}_1^0)$, hence it has a harder jet spectrum. The third mass hierarchy aims at scenarios where $\Delta m(\tilde{t}, \tilde{\chi}_1^{\pm})$ is small, while the fourth hierarchy targets scenarios for which both Δm values are sizeable.

The four signal regions t1L-bCa_low, t1L-bCa_med, t1L-bCb_med1, t1L-bCb_high, have the common feature of making use of a dedicated soft lepton selection. The t1L-bCa signal regions require a hard initial state radiation jet to boost the stop pair system and produce a sizeable amount of missing transverse momentum. The t1L-bCb exploit the presence of two relatively hard b-jets in the event.

The signal region t1L-bCc_diag targets a mass hierarchy complementary to that of the t1L-bCb. The small value of $\Delta m(\tilde{t}, \tilde{\chi}_1^{\pm})$ gives rise to soft b-jets, hence no b-tagged jets are required for this region, but a relatively high-p_{T} lepton arising from the W decay.

Topologies arising from scenarios where both $\Delta m(\tilde{t}, \tilde{\chi}_1^{\pm})$ and $\Delta m(\tilde{\chi}_1^{\pm}, \tilde{\chi}_1^0)$ are sizeable are targeted by the three t1L-bCd regions: they all require four jets in the final state; they are characterised by different b-jet multiplicities and they apply different selections on $E_{\mathrm{T}}^{\mathrm{miss}}$, m_{T} and am_{T2}[3] variables. A veto on additional isolated tracks and loose tau candidates helps in suppressing the dominant SM background from dileptonic $t\bar{t}$ decays.

The last two signal regions in table 1, t1L-3body and t1L-tNbC_mix have been optimised for two additional possible scenarios. If $\Delta m(\tilde{t}, \tilde{\chi}_1^0) < m_{\mathrm{top}}$ and the mass hierarchy or the model parameters suppress the decay through a chargino, then the dominant stop decay is $\tilde{t} \to bW\tilde{\chi}_1^0$, through an off-shell top quark (3-body decay). This dedicated signal region relies on the shape information from the m_{T} and am_{T2} variable distributions. Finally, t1L-tNbC_mix is designed to recover sensitivity in scenarios where the stop is assumed to decay with similar probabilities to $t\tilde{\chi}_1^0$ and $b\tilde{\chi}_1^{\pm}$: the selection aims at rejecting the dominant dileptonic $t\bar{t}$ background by making use of a *topness* variable [45], which is obtained by minimising a χ^2 function indicating the similarity of the event to dileptonic $t\bar{t}$ decay.

[2] The transverse mass m_{T} between the lepton with transverse momentum $\vec{p}_{\mathrm{T}}$ and the missing transverse momentum vector $\mathbf{p}_{\mathrm{T}}^{\mathrm{miss}}$ with magnitude $E_{\mathrm{T}}^{\mathrm{miss}}$ is defined as

$$m_{\mathrm{T}} = \sqrt{2\left(|\vec{p}_{\mathrm{T}}|E_{\mathrm{T}}^{\mathrm{miss}} - \vec{p}_{\mathrm{T}} \cdot \mathbf{p}_{\mathrm{T}}^{\mathrm{miss}}\right)} \tag{1}$$

and it is extensively used in one lepton final states to reject SM background processes containing one W boson decaying leptonically.

[3] The asymmetric stransverse mass variable is a variant of the stransverse mass variable [43, 44] defined to efficiently reject dileptonic $t\bar{t}$ decays. It is assumed that one $W \to l\nu$ boson decay on one leg and the neutrino on the other decay leg go undetected, hence the "asymmetry" in the name.

4 Combination of the t0L and t1L analyses

Both the t0L and the t1L analyses have dedicated signal regions targeting the pair production of stops, followed by the decay into $\tilde{t}_1 \to t\tilde{\chi}_1^0$ with a branching fraction of 100%. Indeed, the expected sensitivity of the two analyses to this decay mode is comparable. The signal region selections are mutually exclusive by definition, hence an appropriate statistical combination of the results is expected to significantly extend the ATLAS sensitivity for such scenarios.

Moreover, both the t0L and the t1L analyses have published exclusion limits for models where the stop is assumed to decay either through $\tilde{t}_1 \to t\tilde{\chi}_1^0$ or $\tilde{t}_1 \to b\tilde{\chi}_1^\pm$ as a function of the branching ratio x of the former, and assuming $m_{\tilde{\chi}_1^\pm} = 2m_{\tilde{\chi}_1^0}$. The two analyses have a comparable sensitivity for large to moderate values of x, while the t1L analysis has a larger sensitivity at small x.

The statistical combination of the two analyses is performed by running the combined fit simultaneously on the control and signal regions of the two analyses. The detector-level systematic uncertainties are treated as correlated by using, for each of the uncertainties considered, one single nuisance parameter. The supersymmetric signal parameter strength used is the same for the two analyses, while the normalisation parameters for the background processes are kept independent in each analyses' control and signal regions[4]. The nuisance parameters associated with modelling uncertainties of the various processes are also kept.

The control regions of the two analyses are not mutually exclusive: the events that belong to both a CR of t0L and one of t1L are, at most about 2% (15%) of the total number of events of the t0L (t1L) CR . The strategy adopted is to remove them from the corresponding t0L CR for the combination. It has been verified that such removal does not affect the individual results of the t0L analysis.

For each combination performed, the fit setup is validated by checking that the background normalisation parameters obtained are compatible with those obtained separately by the two analyses, by verifying that no additional constraint of the nuisance parameters is introduced with respect to the individual fits and by checking that no artificial correlation is introduced between any of the fit parameters.

The first combination is performed targeting a simplified model where the only stop decay is $\tilde{t}_1 \to t\tilde{\chi}_1^0$. For $m_{\tilde{t}_1} < 400$ GeV or $m_{\tilde{t}_1} - m_{\tilde{\chi}_1^0} < 250$ GeV, the t1L analysis outperforms the t0L analysis in terms of sensitivity, hence combining the two is not useful, so the t1L is used in these regions. Otherwise, the set of signal regions in t0L that gives the smallest expected value of the CL_s (among the combination t0L-SRA+t0L-SRB and t0L-SRA+t0L-SRC used in Ref. [23]) is combined with the signal region giving the smallest expected CL_s among t1L-tN_medium and t1L-tN_boost. Figure 2 shows the combined limit of the two analyses. An expected limit about 50 GeV higher in stop mass is achieved at low $m_{\tilde{\chi}_1^0}$ with respect to the individual analyses. The observed limit is increased by roughly the same amount.

A similar combination is performed that targets a scenario where the stop can decay into $\tilde{t}_1 \to t\tilde{\chi}_1^0$ with branching ratio x and into $\tilde{t}_1 \to b\tilde{\chi}_1^\pm$ with branching ratio $1 - x$. The mass of the chargino is assumed to be twice that of the neutralino. Neutralino masses below 50 GeV are not considered, to take into account limits on the lightest chargino mass obtained at LEP [46–50]. The exclusion limits have been derived

[4] The choice is motivated by the fact that the phase space regions in which the two analyses determine the normalisation parameters of the $t\bar{t}$, Z + jets and W + jets (for t0L) and $t\bar{t}$ and W + jets (for t1L) are characterised by different kinematic selections and jet multiplicities.

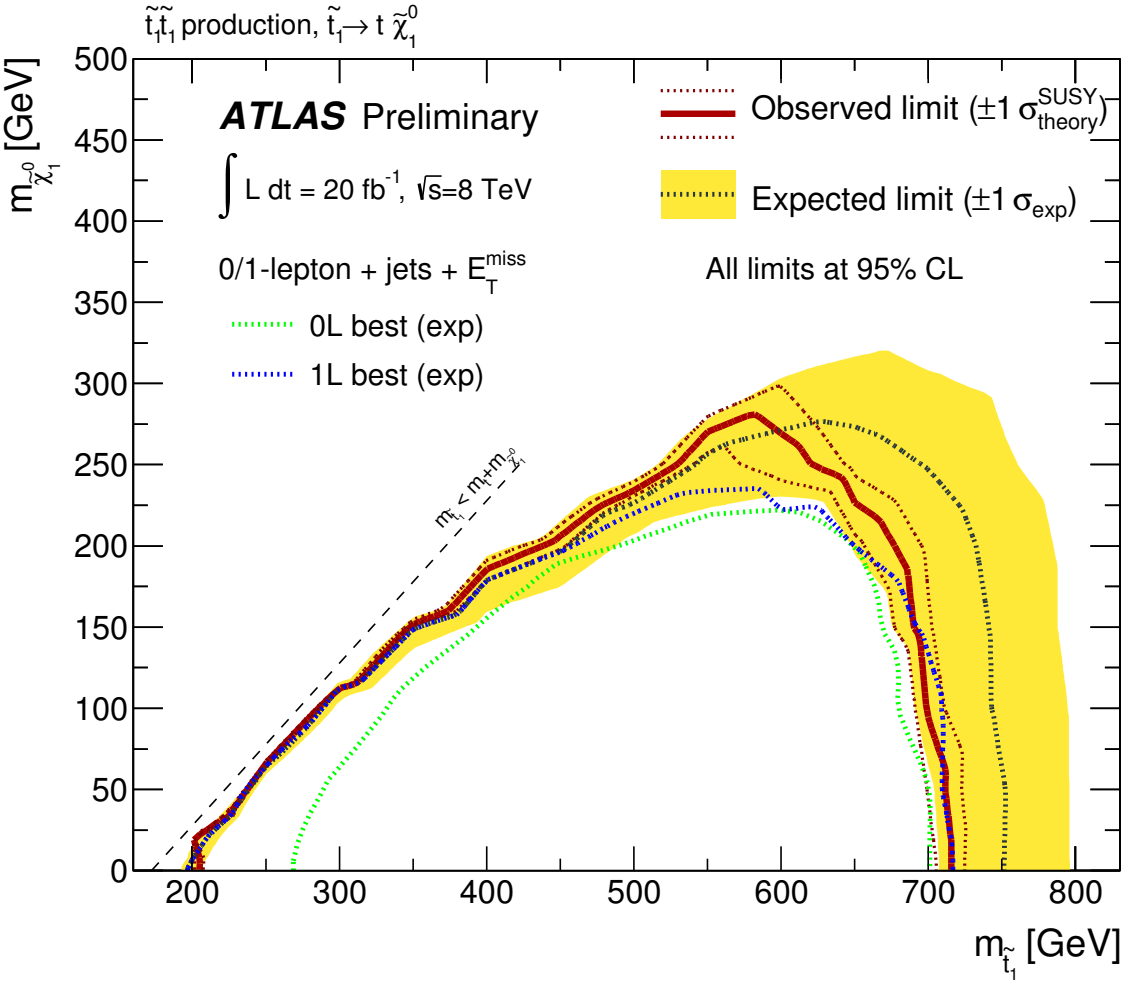

Figure 2: Combined exclusion limits at 95% CL$_s$ in the scenario where both top squarks decay exclusively via $\tilde{t}_1 \rightarrow t\,\tilde{\chi}_1^0$. The black dashed line indicates the expected limit, and the yellow band indicates the $\pm1\sigma$ uncertainties, which include all uncertainties except the theoretical uncertainties in the signal. The red solid line indicates the observed limit, and the red dotted lines indicate the sensitivity to $\pm1\sigma$ variations of the signal theoretical uncertainties. For comparison the dotted green and blue lines show the expected limits from the stand-alone t0L and t1L analyses.

for $x = 75\%, 50\%, 25\%$ and 0[5] . Regardless of the branching ratio considered, it is always assumed that $m_{\tilde{t}_1} > m_t + m_{\tilde{\chi}_1^0}$ and $m_{\tilde{t}_1} > m_b + m_{\tilde{\chi}_1^\pm}$, such that the two decays $\tilde{t}_1 \to t\tilde{\chi}_1^0$ and $\tilde{t}_1 \to b\tilde{\chi}_1^\pm$ are both kinematically allowed. A full statistical combination, identical in setup to the one just described, is used for $x = 75\%$. For smaller values of x, no combined fit is performed, rather either the t0L or the t1L analysis is used, depending which one gives the smallest expected CL_s value.

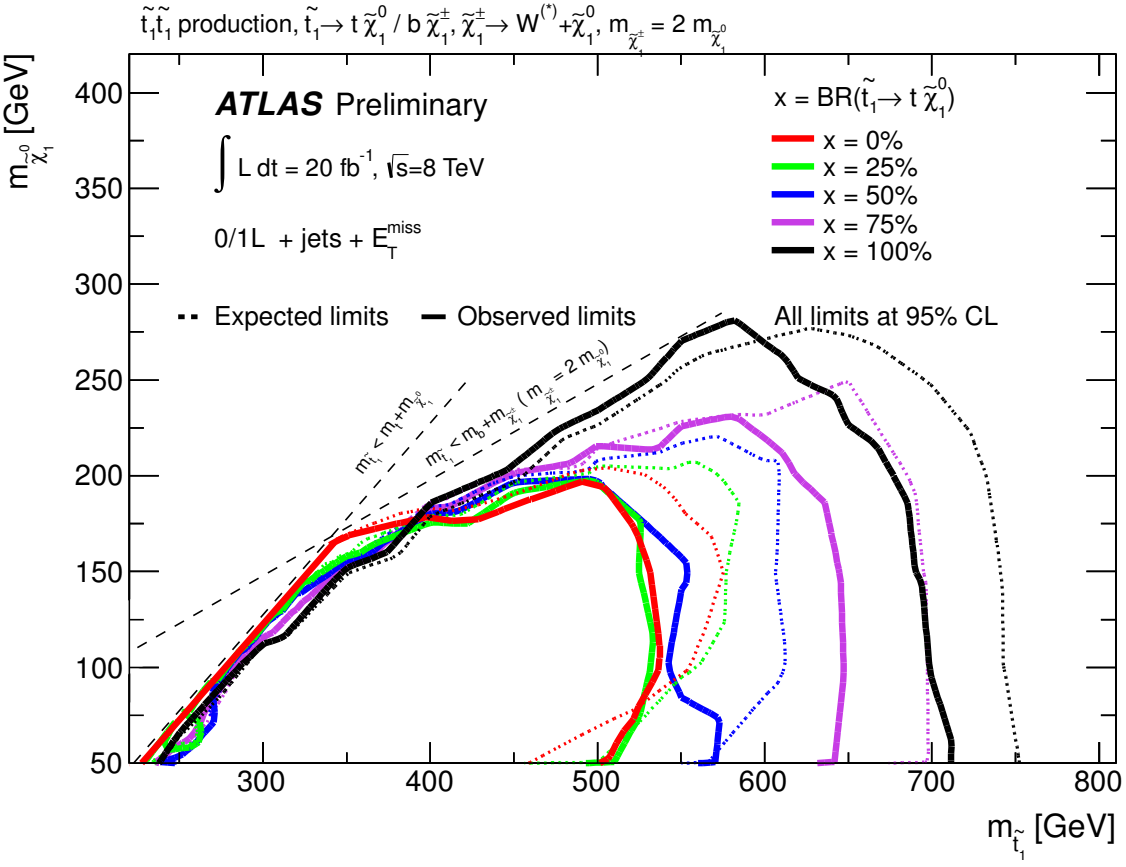

Figure 3: Combined exclusion limits assuming that the stop decays through $\tilde{t}_1 \to t\tilde{\chi}_1^0$ with branching ratio x and through $\tilde{t}_1 \to b\tilde{\chi}_1^\pm$ with branching ratio $1 - x$. The limits assume $m_{\tilde{\chi}_1^\pm} = 2m_{\tilde{\chi}_1^0}$, and values of x from 0% (inner contours) to 100% (outer contours) are considered. For each branching fraction, the observed (with solid lines) and expected (with dashed lines) limits are shown.

Figure 3 shows the result of the combination. The limit is improved, with respect to the individual analyses, by about 50 GeV for $m_{\tilde{\chi}_1^0} = 50$ GeV at $x = 75\%$. For lower x values, the t1L analysis is used on the full plane, with the exception of the region at the highest stop mass for $m_{\tilde{\chi}_1^0} = 50$ GeV at $x = 50\%$ and 25% (this is in fact the reason for the observed limit being closer to the expected one for these curves).

[5] A value of $x = 0$ is not achievable in a supersymmetric model. This value has been nevertheless consider as a limit case in a simplified model.

5 Conclusion

The results from the analyses of Refs. [23] and [24], selecting events containing no leptons and one lepton respectively, have been combined in a common fit. The resulting exclusion limit in a scenario where the stop decays into a top quark and a stable neutralino extends the exclusion limits of the individual analyses by about 50 GeV for large stop masses. Stop masses up to 700 GeV are excluded for small neutralino masses. Exclusion limits derived for a scenario where the stop decays into either $\tilde{t}_1 \to t\tilde{\chi}_1^0$ (with branching fraction x) or $\tilde{t}_1 \to b\tilde{\chi}_1^\pm$ (with branching fraction $1 - x$), where $m_{\tilde{\chi}_1^\pm} = 2m_{\tilde{\chi}_1^0}$ is assumed, are also significantly extended by the combination for $x > 50\%$.

References

[1] H. Miyazawa, Prog. Theor. Phys. **36 (6)** (1966) 1266–1276.

[2] P. Ramond, Phys. Rev. **D 3** (1971) 2415–2418.

[3] Y. Golfand and E. Likhtman, JETP Lett. **13** (1971) 323–326.

[4] A. Neveu and J. H. Schwarz, Nucl. Phys. **B 31** (1971) 86–112.

[5] A. Neveu and J. H. Schwarz, Phys. Rev. **D 4** (1971) 1109–1111.

[6] J. Gervais and B. Sakita, Nucl. Phys. **B 34** (1971) 632–639.

[7] D. Volkov and V. Akulov, Phys. Lett. **B 46** (1973) 109–110.

[8] J. Wess and B. Zumino, Phys. Lett. **B 49** (1974) 52–54.

[9] J. Wess and B. Zumino, Nucl. Phys. **B 70** (1974) 39–50.

[10] S. Weinberg, Phys. Rev. **D 13** (1976) 974–996.

[11] E. Gildener, Phys. Rev. **D 14** (1976) 1667–1672.

[12] S. Weinberg, Phys. Rev. **D 19** (1979) 1277–1280.

[13] L. Susskind, Phys. Rev. **D 20** (1979) 2619–2625.

[14] R. Barbieri and G. Giudice, Nucl. Phys. **B 306** (1988) 63–76.

[15] B. de Carlos and J. Casas, Phys. Lett. **B 309** (1993) 320–328, arXiv:hep-ph/9303291 [hep-ph].

[16] P. Fayet, Phys. Lett. **B 64** (1976) 159–162.

[17] P. Fayet, Phys. Lett. **B 69** (1977) 489–494.

[18] G. R. Farrar and P. Fayet, Phys. Lett. **B 76** (1978) 575–579.

[19] P. Fayet, Phys. Lett. **B 84** (1979) 416–420.

[20] S. Dimopoulos and H. Georgi, Nucl. Phys. **B 193** (1981) 150–162.

[21] ATLAS Collaboration,, JINST **3** (2008) S08003.

[22] CMS Collaboration, S. Chatrchyan et al., JINST **3** (2008) S08004.

[23] ATLAS Collaboration,, JHEP **09** (2014) 015, arXiv:1406.1122 [hep-ex].

[24] ATLAS Collaboration,, arXiv:1407.0583 [hep-ex].

[25] ATLAS Collaboration,, JHEP **1406** (2014) 124, arXiv:1403.4853 [hep-ex].

[26] ATLAS Collaboration,, arXiv:1407.0608 [hep-ex].

[27] ATLAS Collaboration,, Eur.Phys.J. **C74** (2014) 2883, arXiv:1403.5222 [hep-ex].

[28] ATLAS Collaboration,, JHEP **1310** (2013) 189, arXiv:1308.2631 [hep-ex].

[29] ATLAS Collaboration,, Phys. Lett. **B 715** (2012) 44–60, arXiv:1204.6736 [hep-ex].

[30] ATLAS Collaboration,, Phys. Rev. Lett. **109** (2012) 211802, arXiv:1208.1447 [hep-ex].

[31] ATLAS Collaboration,, Eur. Phys. J. **C 72** (2012) 2237, arXiv:1208.4305 [hep-ex].

[32] ATLAS Collaboration,, JHEP **11** (2012) 094, arXiv:1209.4186 [hep-ex].

[33] ATLAS Collaboration,, Phys. Lett. **B 720** (2013) 13–31, arXiv:1209.2102 [hep-ex].

[34] CMS Collaboration,, Phys. Rev. Lett. **111** no. 8, (2013) 081802, arXiv:1212.6961 [hep-ex].

[35] CMS Collaboration,, JHEP **01** (2013) 077, arXiv:1210.8115 [hep-ex].

[36] CMS Collaboration,, Eur. Phys. J. **C 73** (2013) 2568, arXiv:1303.2985 [hep-ex].

[37] CMS Collaboration,, Eur. Phys. J. **C 73** (2013) 2677, arXiv:1308.1586 [hep-ex].

[38] CMS Collaboration,, Phys. Rev. Lett. **112** (2014) 161802, arXiv:1312.3310 [hep-ex].

[39] M. Baak, G. Besjes, D. Cote, A. Koutsman, J. Lorenz, et al., arXiv:1410.1280 [hep-ex].

[40] G. Cowan, K. Cranmer, E. Gross, and O. Vitells, Eur.Phys.J. **C71** (2011) 1554, arXiv:1007.1727 [physics.data-an].

[41] T. Junk, Nucl.Instrum.Meth. **A434** (1999) 435–443, arXiv:hep-ex/9902006 [hep-ex].

[42] A. L. Read, J.Phys. **G28** (2002) 2693–2704.

[43] C. Lester and D. Summers, Phys. Lett. **B 463** (1999) 99–103, arXiv:hep-ph/9906349.

[44] A. Barr, C. Lester, and P. Stephens, J.Phys. **G29** (2003) 2343–2363, arXiv:hep-ph/0304226 [hep-ph].

[45] M. L. Graesser and J. Shelton, Phys.Rev.Lett. **111** no. 12, (2013) 121802, arXiv:1212.4495 [hep-ph].

[46] lep susy working group (aleph, delphi, l3, opal), notes lepsusywg/01-03.1 and 04-02.1, http://lepsusy.web.cern.ch/lepsusy/welcome.html.

[47] ALEPH Collaboration, A. Heister et al., Phys. Lett. **B 583** (2004) 247–263.

[48] DELPHI Collaboration, J. Abdallah et al., Eur. Phys. J. **C 31** (2003) 421–479, arXiv:hep-ex/0311019 [hep-ex].

[49] L3 Collaboration, M. Acciarri et al., Phys. Lett. **B 472** (2000) 420–433, arXiv:hep-ex/9910007 [hep-ex].

[50] OPAL Collaboration, G. Abbiendi et al., Eur. Phys. J. **C 35** (2004) 1–20, arXiv:hep-ex/0401026 [hep-ex].